Remote Sens. **2013**, *5*, 1603-1623; doi:10.3390/rs5041603

OPEN ACCESS

Remote Sensing

ISSN 2072-4292

www.mdpi.com/journal/remotesensing

Article

Evaluation of Soil Moisture Retrieval from the ERS and Metop Scatterometers in the Lower Mekong Basin

Vahid Naeimi [1,2,*], Patrick Leinenkugel [2], Daniel Sabel [3], Wolfgang Wagner [3], Heiko Apel [4] and Claudia Kuenzer [2]

[1] Department of Remote Sensing, University of Würzburg, Am Hubland, 97074 Würzburg, Germany

[2] German Remote Sensing Data Center (DFD), German Aerospace Center (DLR), Münchener Str. 20, 82234 Wessling, Germany; E-Mails: patrick.leinenkugel@dlr.de (P.L.); claudia.kuenzer@dlr.de (C.K.)

[3] Research Group Remote Sensing, Department of Geodesy and Geoinformation (GEO), Vienna University of Technology, Gusshaus Str. 27-29, 1040 Vienna, Austria; E-Mails: ds@ipf.tuwien.ac.at (D.S.); ww@ipf.tuwien.ac.at (W.W.)

[4] Section 5.4: Hydrology, GFZ German Research Centre for Geoscience, Telegrafenberg, 14473 Potsdam, Germany; E-Mail: heiko.apel@gfz-potsdam.de

* Author to whom correspondence should be addressed; E-Mail: vahid.naeimi@dlr.de; Tel.: +49-8153-28-2460; Fax: +49-8153-28-1458.

Received: 5 February 2013; in revised form: 20 March 2013 / Accepted: 21 March 2013 / Published: 27 March 2013

Abstract: The natural environment and livelihoods in the Lower Mekong Basin (LMB) are significantly affected by the annual hydrological cycle. Monitoring of soil moisture as a key variable in the hydrological cycle is of great interest in a number of Hydrological and agricultural applications. In this study we evaluated the quality and spatiotemporal variability of the soil moisture product retrieved from C-band scatterometers data across the LMB sub-catchments. The soil moisture retrieval algorithm showed reasonable performance in most areas of the LMB with the exception of a few sub-catchments in the eastern parts of Laos, where the land cover is characterized by dense vegetation. The best performance of the retrieval algorithm was obtained in agricultural regions. Comparison of the available *in situ* evaporation data in the LMB and the Basin Water Index (BWI), an indicator of the basin soil moisture condition, showed significant negative correlations up to R = −0.85. The inter-annual variation of the calculated BWI was also found corresponding to the reported extreme hydro-meteorological events in the Mekong region. The retrieved

soil moisture data show high correlation (up to R = 0.92) with monthly anomalies of precipitation in non-irrigated regions. In general, the seasonal variability of soil moisture in the LMB was well captured by the retrieval method. The results of analysis also showed significant correlation between El Niño events and the monthly BWI anomaly measurements particularly for the month May with the maximum correlation of R = 0.88.

Keywords: soil moisture; Scatterometer; ASCAT; Mekong

1. Introduction

The Mekong River is the longest river in Southeast Asia and the world's eighth largest in discharge draining an area of 795,000 km². It flows through six states in Southeast Asia and drains a pan-shaped basin to the South China Sea (Figure 1). The upper part of the basin consists of mountainous terrain and is referred to as Upper Mekong Basin. In the lower remaining portion of the basin, Lower Mekong Basin (LMB), the Mekong River has several tributaries with a drainage area of 606,000 km² within Laos, Thailand, Cambodia and Vietnam [1,2]. The LMB is considered as the most important part of the Mekong basin, both socio-economically and environmentally [3]. Millions of people living in different geographical areas of the LMB rely on the river system for their livelihoods. The livelihoods and food security of most people in many parts of the LMB are tightly dependent on water resources which this makes the life of people highly vulnerable to availability and quality of the resources. The flat terrains in the LMB are used for crop irrigation, animal raising and fish farm operations. About 80–90% of all water from the Mekong River is used for agriculture, most of which for crop cultivation [4]. "The rapid population growth and socioeconomic development in the Mekong region over the past several decades has been accompanied by extensive deforestation, expansion of agriculture and irrigation, and stream-flow regulation" [5]. Furthermore, extensive hydropower developments along the Mekong River main stem and its tributaries are built for irrigation and energy supply, causing basin wide effects on annual water flow and sediment load cycles [6]. The riparian people and the ecosystem of the Mekong basin are strongly affected by the river's annual cycle of rainy and dry season and the hydrologic cycle plays a fundamental role in maintaining the health of the Mekong Basin environment.

Soil moisture is a key variable in the hydrologic cycle over timescales ranging from hourly to inter-annual. It functions as a link between the energy and water fluxes at the soil surface and the atmosphere interface. The local and regional hydrological processes, partitioning of precipitation into infiltration and runoff as well as the availability of water to plants and so also the partitioning of latent and sensible heat are influenced and controlled by soil moisture [7]. Furthermore, soil moisture has been recognized as an essential variable in the climate system [8]. It is, along with snow, the most important component of meteorological memory over land [9]. Soil moisture and the memory associated with it have important roles in the feedback mechanisms that intensify and prolong climate anomalies [10]. Knowledge of soil moisture variations is valuable for understanding the hydrological cycle and predicting extreme events and their impacts on environment, climate change and weather forecasting [11].

Figure 1. Maps of the Mekong Basin: (**a**) river network; (**b**) topography; and (**c**) main catchments in the Lower Mekong Basin.

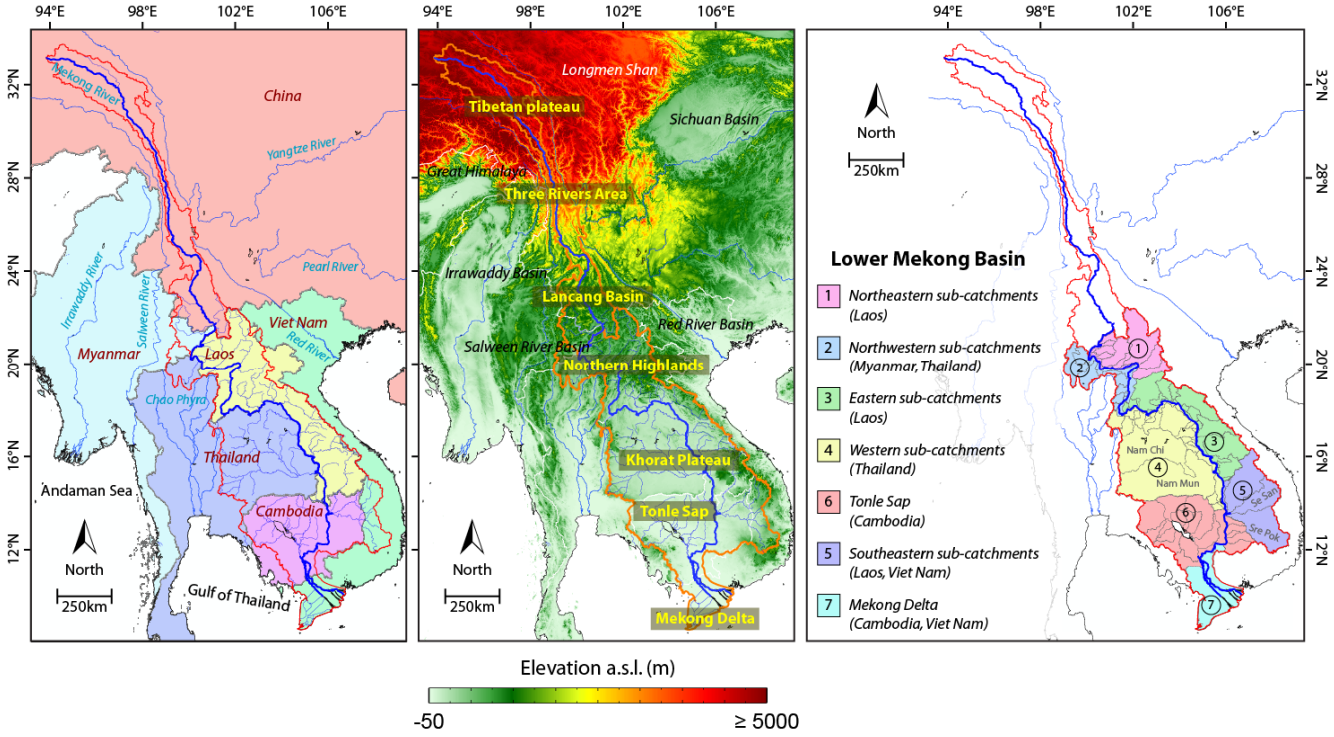

Surface soil moisture has high spatial and temporal variability, which makes the ground-truth measurement very difficult. The *in situ* measurements are precise but basically point measurements. A large number of samples must be taken to determine the regional variability of soil moisture. Hence, applying remote sensing techniques are very practical for monitoring of soil moisture dynamics providing frequent measurements (up to twice a day in case of scatterometer) over large areas. Remote sensing techniques have also the advantage of averaging within-pixel variability which masks the underlying land surface heterogeneity [12]. Microwave remote sensing specially in the low frequency domain (1–10 GHz) offers a relatively direct method of soil moisture retrieval thanks to the strong relationship between the moisture content and dielectric constant of the soil [13]. The microwave remote sensing methods are limited to shallower soil depth compared to *in situ* measurement because of limited penetration depth of the low frequency microwaves (1~5 cm). Nevertheless, an appropriate infiltration model can be applied for estimation of the profile soil moisture from surface observations.

In this study we used scatterometer-derived soil moisture data for determination of soil moisture variability in the LMB. The two main objectives of this study were to investigate the overall quality of the scatterometer derived soil moisture in the Mekong Basin and characterization of the catchment-based soil moisture variability in the LMB. A brief overview of the study region is given in Section 2 followed by the descriptions of the datasets used in this study in Section 3. Section 4 describes the methodology and retrieval procedure of the soil moisture data. Section 5 presents the results of the analysis divided in three main sub-sections: the quality assessment of the scatterometer soil moisture (SSM) product through the SSM uncertainty analysis, comparison of the SSM data with hydro-meteorological observations, and descriptive analysis of the SSM spatiotemporal variability in the LMB.

2. Study Area

The study area is limited to the Lower Mekong Basin (LMB), where the Mekong's major tributaries are located. The Lower Mekong Basin contains the Northern Highlands, the Khorat Plateau, the Tonle Sap Basin and the Mekong Delta. Figure 1-right shows the LMB's sub-catchments, which put together the major physiographic sub-regions. The "Northern Highlands" with elevations of up to about 2,800 m comprise the northern parts of Thailand and Laos, the upland region of northeast Myanmar, and eastward into the northern end of the Annamite Range in Vietnam. The Northern Highlands region receives the highest amount of rainfall in the LMB. The "Khorat Plateau" is bound to the northeastern region of Thailand and the Annamite Mountains to the east and northeast. The Khorat Plateau is the driest region in the LMB with the highest evapotranspiration rate despite the annual rainfall between 1,000 to 1,600 mm [2]. The "Tonle Sap" Basin, situated in Cambodia, is the catchment area of the Tonle Sap River at its confluence with the Mekong River. The western and central parts of the Tonle Sap Basin form a low-relief region in which the Tonle Sap Lake, the largest freshwater lake in Southeast Asia, is located. The "Mekong Delta" is defined as the flat region in southwestern Vietnam where the Mekong River approaches and drains into the sea through a vast network of natural distributaries and man-made channels. The climate of the Mekong Basin is strongly influenced by the rainy southwest monsoon occurring between May and October and dry northeast monsoon in the period of October-March. Therefore rainfall is strongly seasonal. About 90% of precipitation falls between the months of May and October with mean annual totals ranging from 1,000 mm in northeast Thailand to more than 3,200 mm in the mountainous regions of Laos [14]. The hydrologic cycle in the LMB is dominated by a single-wet-season flow peak. Annual floods in the Mekong Basin are characterized as natural occurrences with a distinct peak and large amplitude, bringing fertile and nutrients-rich sediments [15].

3. Data

3.1. Scatterometer-Derived Soil Moisture Product

The scatterometer soil moisture (SSM) product used in this study is retrieved from C-band (5.3 GHz) active sensors aboard European Remote Sensing Satellites (ERS-1&2) [16] and the first Meteorological Operation (Metop-A) satellite [17] by using the TUWien soil moisture retrieval algorithm developed at the Vienna University of Technology [18,19]. The SSM product generation is carried out by employing two sets of model parameters, extracted separately from backscatter time series measured by the scatterometers onboard ERS-1&2 (SCATs) and the advanced scatterometer (ASCAT) onboard Metop-A. The Metop-A is the first of three foreseen meteorological satellites planned by the European Organization for the Exploitation of Meteorological Satellites (EUMETSAT). The SCATs data acquisitions in the Mekong river basin are available from August 1991 to January 2001 with a spatial resolution of about 50 km and daily coverage of about 40%. The backscatter measurements of the ASCAT, the successor of SCATs, are available in two different spatial resolutions of 25 km and 50 km since January 2007 [20]. The ASCAT has double daily spatial coverage with respect to its predecessor SCAT. In the TUWien processing algorithm, the backscatter measurements from SCATs (50 km) and ASCAT (25 km) are re-sampled from the satellite orbit into a

Discrete Global Grid (DGG) with 12.5 km grid spacing. The outcome of this procedure, which has been used throughout the study, is the backscatter time series covering from 1991 to 2011 with a gap between 2001 and 2007. Although the quality of SSM retrieved from SCAT and ASCAT measurements depends highly on the relative radiometric accuracy and calibration of the two generations of instruments, it was shown that the overall consistency of the combined dataset is satisfying [21].

3.2. Hydro-Meteorological Data

Since no *in situ* soil moisture measurements in the LMB were available for this study, *in situ* evaporation and reanalysis precipitation data have been used for indirect quality assessment of the SSM product.

3.2.1. Evaporation *in situ* Data

The Mekong River Commission (MRC) collects a variety of hydro-meteorological *in situ* measurements within the LMB from the national hydro-meteorological agencies of the member states. The MRC database is available through the MRC Master Catalogue [22]. The actual evaporation data have been collected from 68 stations within the LMB available in the period of 1992–2011.

3.2.2. Reanalysis Precipitation Data

The Global Precipitation Climatology Centre (GPCC) provides monthly precipitation and relative climatological normal produced based on long-term *in situ* rain-gauge observations. In this study, the full reanalysis product with the spatial resolutions of 0.5° × 0.5° is used which was generated using the complete GPCC monthly rainfall station database covering the period from 1901 to 2010 [23,24]. The GPCC products are freely available from http://gpcc.dwd.de.

4. Method

4.1. TUWien Soil Moisture Retrieval Algorithm

The TUWien soil moisture retrieval algorithm is based on change detection of the normalized radar cross section (σ^0) measured by the SCAT and ASCAT scatterometers. Two distinct parameter databases were used for processing of the backscatter data extracted separately from SCAT and ASCAT backscatter time series. The multi-looking direction ability of the scatterometers is utilized to describe the incidence angle behavior of the backscatter as a seasonal function. Then the estimated incidence-angle dependency function is used for normalization of the σ^0 to a reference incidence angle chosen as 40° and also to remove vegetation contribution in the σ^0 measurements. Once the incidence angle dependency is removed, it can be assumed that there is a linear relationship between the variations in soil water content and σ^0 expressed in decibel [13]. Eventually, the normalized backscatter σ_{40} is scaled between the lowest and the highest values ever measured over a given geographical location within the long-term σ_{40} observations representing the driest and wettest conditions. In this way, the corresponding surface soil moisture saturation index at topmost soil surface

is extracted ranging between 0% and 100% [18,19]. The TUWien soil moisture retrieval method has been used and validated in numerous studies (e.g., [25–34]).

4.2. TUWien Soil Moisture Retrieval Uncertainty

In parallel to the SSM retrieval, an error analysis is carried out within the TUWien processing algorithm to determine uncertainties associated with the measurements and the model parameters. The TUWien error propagation is initialized with a so-called Estimated Standard Deviation of backscatter (ESD), which represents azimuthal noise caused by surface anisotropy. The ESD is calculated using concurrent backscatter measurements from the fore and aft beam antennas at the same incidence angle but from two different azimuthal directions [35]. Using the TUWien error propagation procedure, the uncertainties in the measured variables are carried over to determine the final SSM uncertainty. The noise of soil moisture retrieved from the scatterometer data comprises errors coming from the instrument, azimuthal anisotropy, speckle, as well as the uncertainties associated with the model parameters. The calculated SSM noise is an indicator of the TUWien model performance [19].

4.3. Basin Water Index (BWI)

The soil moisture product retrieved from scatterometer data provides information about the top soil surface as the penetration depth of the C-band microwaves in the soil is only about 1–3 cm, while knowledge of soil water content in the plant root zone is of interest to many hydrological and agricultural applications. The land surface components of the hydrological cycle behave in different time scales. Depending on vegetation-soil system, different water reservoirs have different time scales; very short time scale for canopy water, intermediate for surface soil moisture, and long term scale for root zone soil moisture [36]. The moisture contained within the surface soil layer and root zone interact via the process of infiltration. Wagner *et al*. [18] proposed a simple method for estimation of profile soil moisture using surface soil moisture measurements. The method is based on a simple infiltration model to extract a so-called Soil Water Index (SWI). The Soil Water Index (SWI) is calculated from temporally irregular SSM measurements using the following formulation:

$$SWI(t_n) = \frac{\sum_{i}^{n} SSM(t_i)\ e^{-\frac{t_n - t_i}{T}}}{\sum_{i}^{n} e^{-\frac{t_n - t_i}{T}}} \quad for\ \ t_i \le t_n \tag{1}$$

where SSM is the surface soil moisture, t is the time of measurements and T is a time characteristic parameter linking SWI with the observation depth according to T = L/C where L is the depth of reservoir layer and C is an area-representative pseudeo-diffusivity constant. In this study T has been chosen as 20.

The above formulation assumes a two-layer water balance model, with the first layer representing the soil surface layer accessible to C-band scatterometer and the second layer as the part of the profile which extends downwards from the bottom of the soil surface layer. It is assumed that the water content of the lower layers is solely controlled by the past moisture conditions in the surface layer and

thus the precipitation history. In order to obtain a representative indicator of soil moisture conditions across the basin, SWI measurements are aggregated according to the following equation:

$$BWI = \frac{\sum_{i}^{N} SWI_{gp(i)}}{N} \quad (2)$$

where N is the number of grid points (gp) within the basin boundaries.

5. Results and Discussion

This section presents first a quality assessment of the SSM based on the soil moisture retrieval performance in the studied region, followed by ground-truthing of the SSM with hydro-meteorological data, and finally an evaluation of the SSM in terms of spatial and temporal patterns all over the LMB.

5.1. Quality Assessment of the SSM Retrieval

The C-band active sensors have been demonstrated to be suitable instruments for change detection of soil moisture independent to solar illumination and cloud cover [37]. However, the intensity of the backscatter signal is also affected by surface roughness, vegetation structure, and vegetation water content. All these factors influence σ^0 at different time scales. At the end the degree of accuracy and reliability of the soil moisture product will depend on the sensitivity of backscatter to the soil surface, the backscatter measurement noise, and the functionality of the retrieval algorithm. Figure 2(a) shows the backscatter sensitivity of the ERS scatterometer in Southeast Asia. Sensitivity is the range between the highest and lowest backscatter measurements, which varies mainly depending on the fraction of area covered by vegetation and the vegetation architecture (size, shape, and orientation of trunks, branches, and foliage). Backscatter has the lowest sensitivity to changes at the soil surface in very densely vegetated area like rainforest, where the penetration of the C-band signal is limited and therefore the majority of backscatter comes from the vegetation canopy. The lowest sensitivity in Southeast Asia is evident in Central Vietnam and parts of Laos, northern Myanmar, southwest Cambodia and the southern part of Thailand where dense vegetation dominates (e.g., Thorn forest, evergreen forest).

Figure 2(b) shows the Estimated Standard Deviation of backscatter (ESD) and Figure 2(c) shows the mean of the estimated SSM noise in Southeast Asia. The estimated SSM noise can be used to identify areas where the algorithm has the lowest performance. This includes areas with dense vegetation cover, sand deserts, coastal areas, water bodies, areas covered with permanent snow or ice, and areas with complex topography. Figure 3 shows the range and magnitude of the SSM noise averaged for different land cover types based on GLC2000 land cover data [38] in Southeast Asia. However, because of the large footprint size of the scatterometer sensor, the impact of land cover on the SSM noise is not very clear in areas that are characterized by a mixture of different classes of land cover. The highest uncertainty in the soil moisture retrieval occurs when the soil surface is partly covered with water because retrieval is not possible over water bodies. Backscattering from water depends on roughness of the water surface. When the water surface is calm then specular reflection occurs and σ^0 is the lowest. The large water reservoirs, shallow bodies of water like swamps, marshes, estuaries, rivers and any set of small bodies of water increases the soil moisture noise depending on the

water extent compared to the spatial resolution of the scatterometer. However, the magnitude of backscatter noise can be moderated in presence of vegetation as it is the case in swamp areas in the LMB. In the Mekong river basin, the effect of water on SSM retrieval is becoming critical during the flooding season. The structural properties of the surface and the three dimensional architecture of vegetation have also a clear influence on the backscatter sensitivity and SSM retrieval uncertainty. In general, backscatter from the land surfaces covered by vegetation is governed by the scattering properties of the geometrical elements that can be considered to be made up of vegetation, soil surface and the interaction between the vegetation volume and soil surface in the form of multiple scattering [39–42]. The highest sensitivity and therefore lowest uncertainty in the SSM retrieval is obtained in agricultural regions, shrubs and grasslands. The quality of soil moisture retrieval is degraded over anisotropic surfaces, which could be classified as Barren, Gravels, or even Savannas.

The quality of the SSM retrieval is also affected in areas with complex topography. If the look direction of the sensor becomes perpendicular to the orientation of surface feature, a large portion of incident energy will be reflected back to the sensor. The more oblique look direction in relation to the feature orientation, the less energy will be returned to the sensor. Therefore complex topography can significantly increase the azimuthal noise. The areas with complex topography can be identified by the standard deviation of elevation. Figure 4 (right) indicates the normalized standard deviation of elevation in Southeast Asia based on GTOPO30 digital elevation model data [43]. Scatterplots in Figure 4 show the increasing of the averaged SSM noise with intensifying the degree of topographic complexity.

Figure 2. (**a**) Sensitivity of the backscatter signal; (**b**) Estimated Standard Deviation (ESD) of the backscatter signal; (**c**) Mean of the TUWien soil moisture retrieval noise.

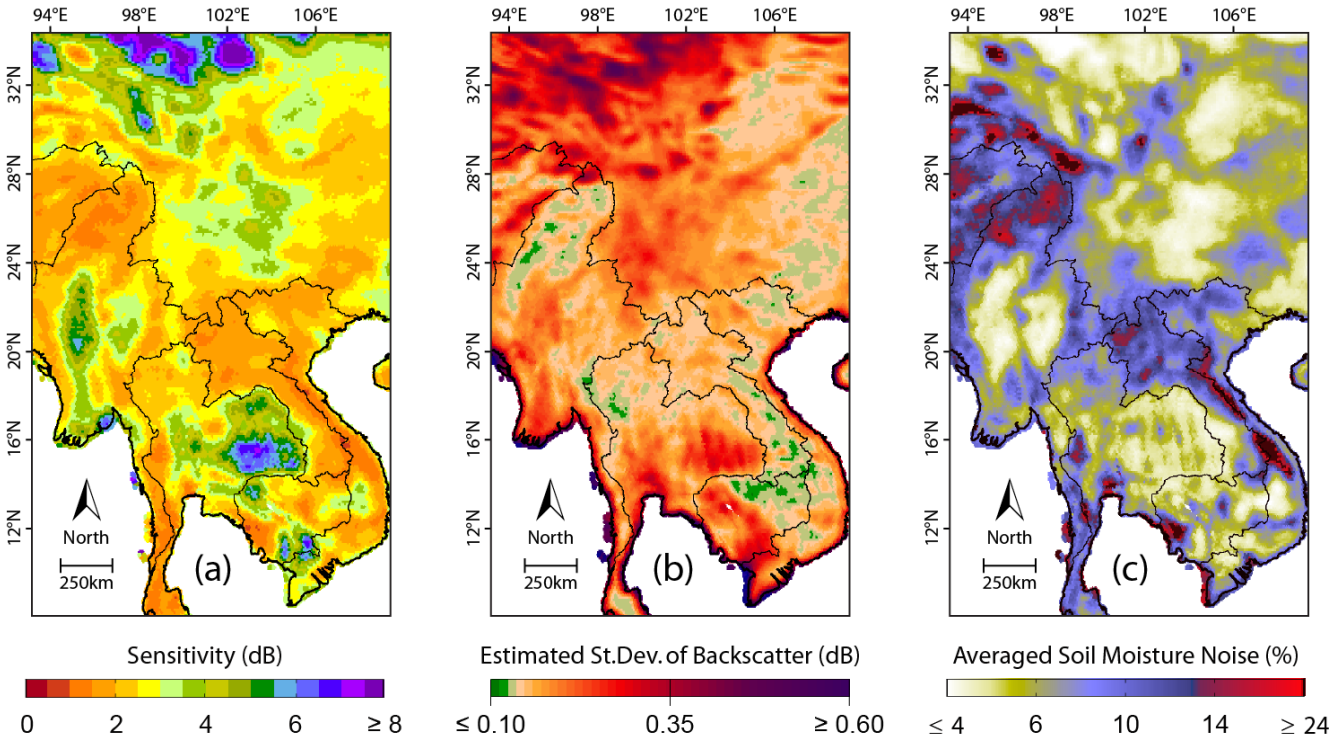

Figure 3. Soil moisture retrieval noise in Southeast Asia averaged over land cover classes.

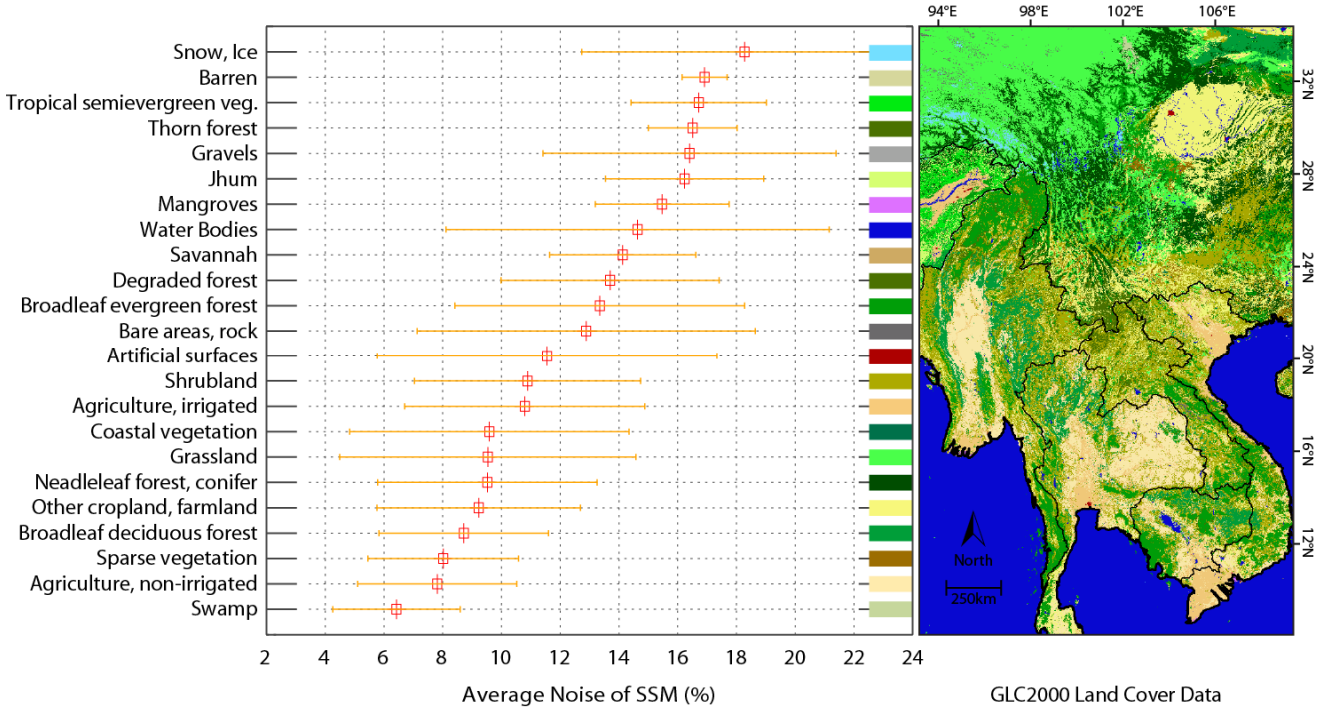

Figure 4. The scatterometer soil moisture (SSM) noise *versus* the topographic complexity in different land cover classes.

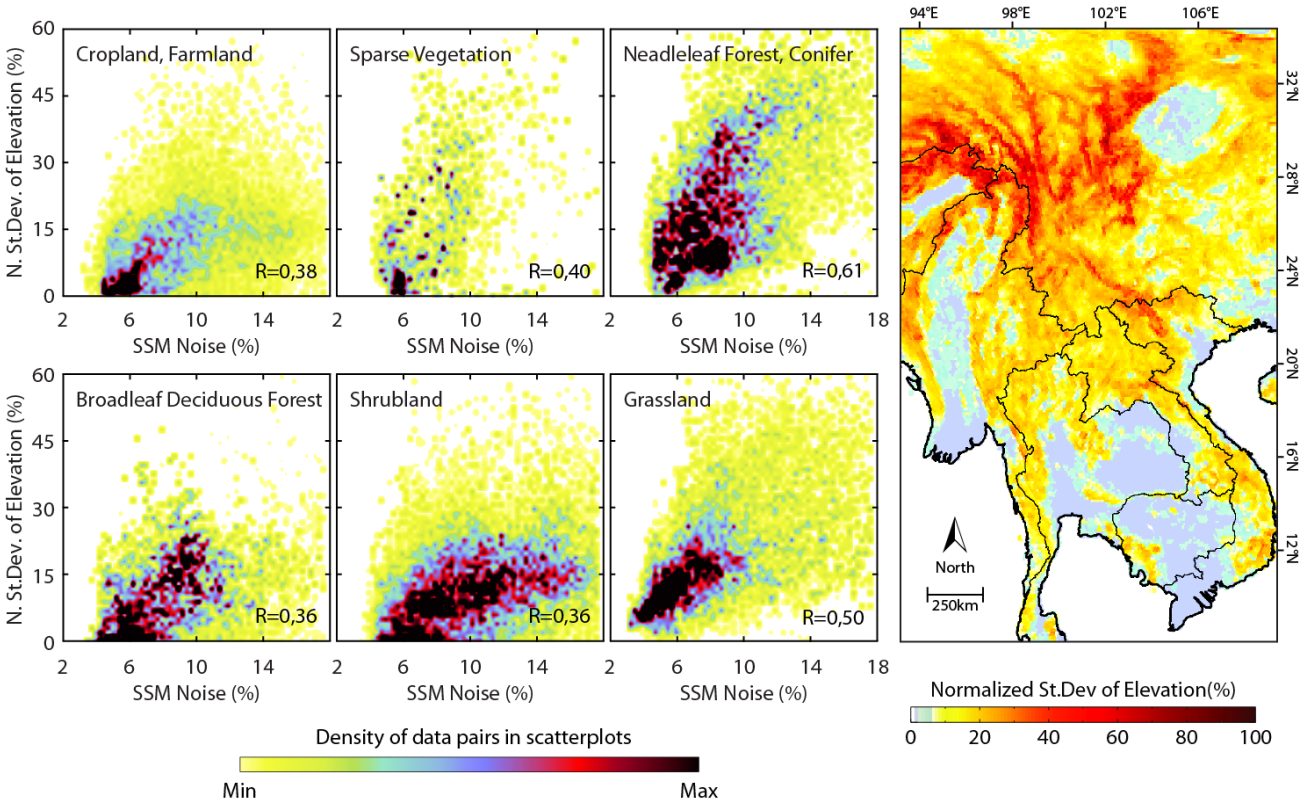

5.2. Comparison of the SSM with Hydro-Meteorological Data

Soil moisture is connected to precipitation and evapotranspiration through water balance equation. The rate of soil moisture (Θ) change is described as the balance between precipitation (P), evapotranspiration (E) and run off (R) [44]:

$$\frac{d\Theta(t)}{dt} = -E + P - R \tag{3}$$

Although the soil moisture is not solely controlled by evaporation, a negative correlation between evaporation and soil moisture is expected in humid regions [45]. Figure 5 shows time series of the SSM compared to the *in situ* evaporation data at three different stations in the LMB. The results of comparison reveal a significant linear relationship between the SSM and the evaporation across the basin with the most significant correlation of R = −0.85 at Se San sub-catchment in Vietnam. Figure 6 shows the results of analysis for all available evaporation measuring stations. It is shown that the inverse correlation was intensified in wet season after excluding the measurements during the flooding period most evidently in Khorat plateau and Delta region.

Figure 5. Examples of the SSM time series compared with the Mekong River Commission (MRC) *in situ* data.

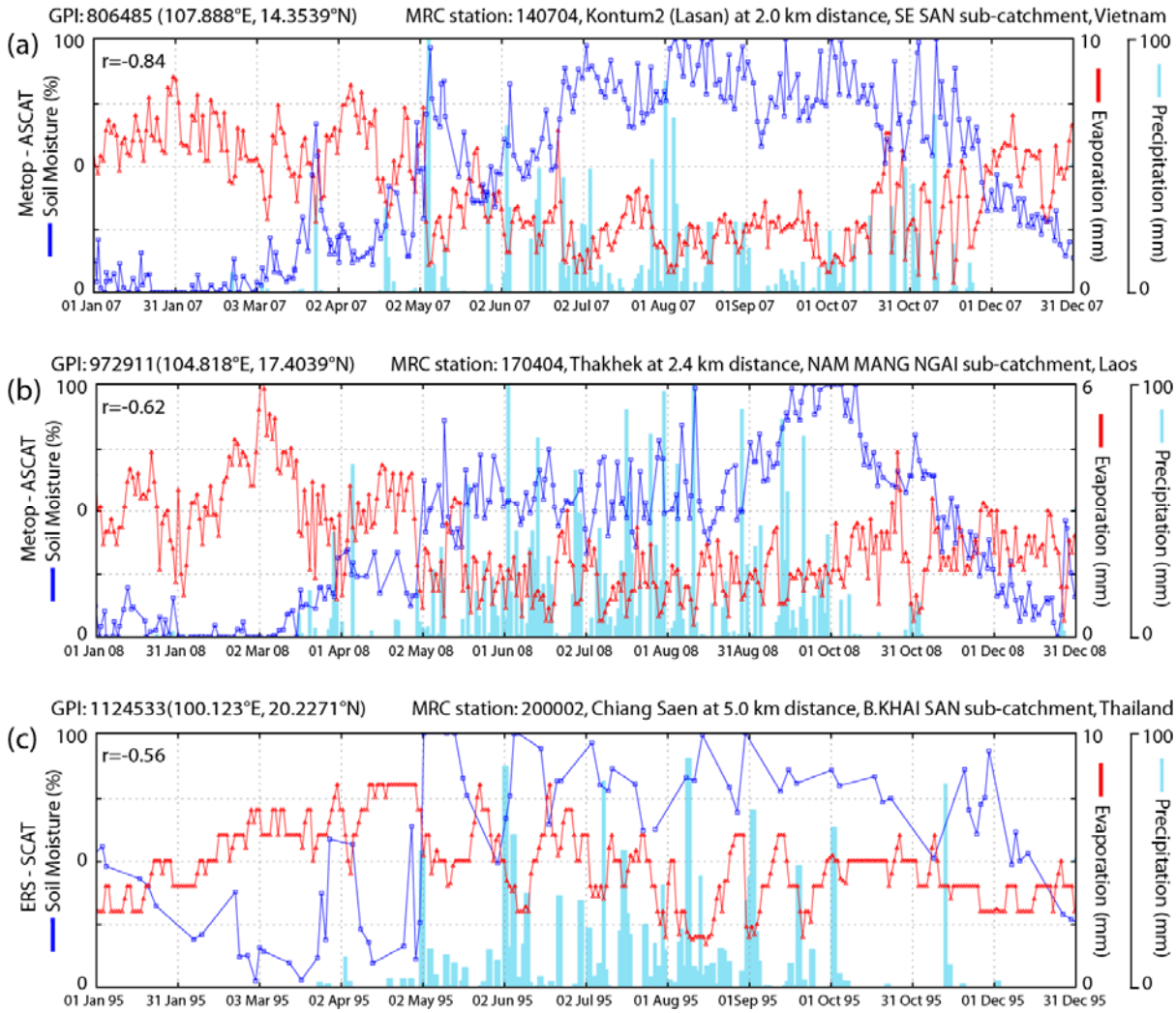

Figure 6. Comparison results of the SSM with *in situ* evaporation data.

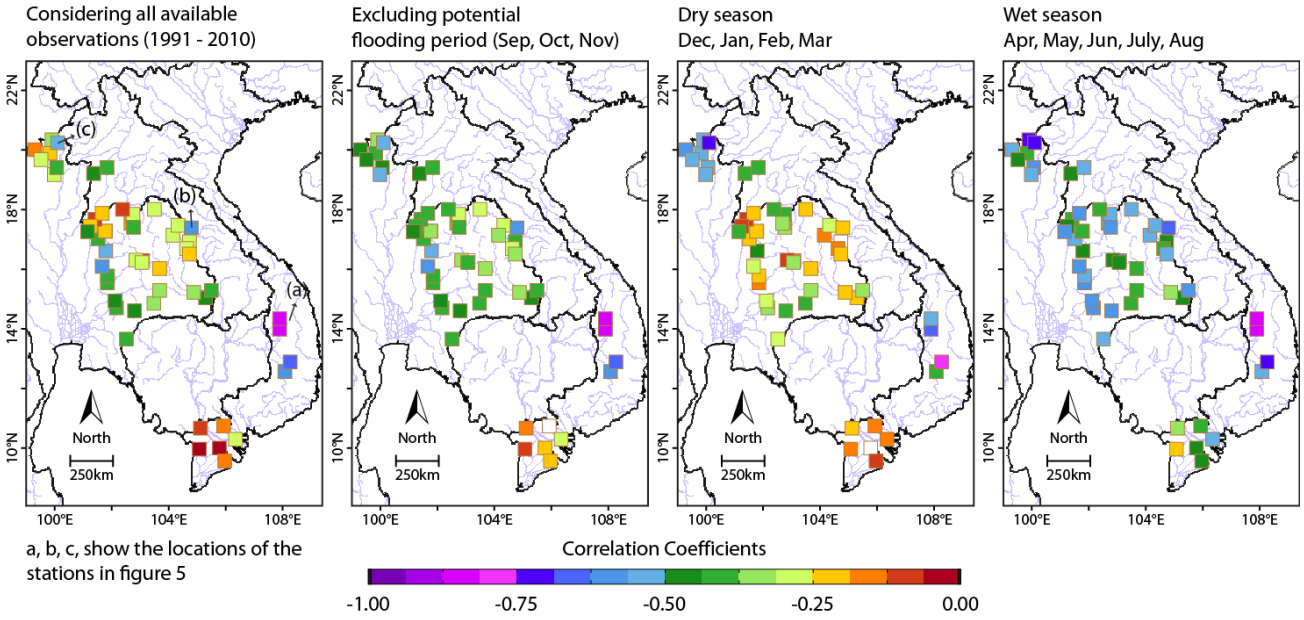

Soil moisture variation due to evaporation, runoff and precipitation occurs on different time scales influenced by soil physical properties and vegetation. Soil texture and structure determine pore size distribution in the soil and therefore they are important factors in determining the rate of water movement in unsaturated soil [46]. Vegetation type and density have also impact on soil water storage dynamics due to different evapotranspiration patterns. Nevertheless, considering the water balance equation, soil moisture increases when precipitation or irrigation exceed evaporation, evapotranspiration and run off. Figure 7 shows three examples of monthly GPCC compared to weekly composites of SSM indicating a noticeable relation between soil moisture and precipitation. Although the total soil water content depends on sum of input precipitation and output evaporation and run off, it is expected that precipitation anomalies are reflected in soil moisture observations. Figure 8 indicates the results of correlation analysis between GPCC monthly anomalies and SSM monthly composites.

Figure 7. Comparison of the monthly Global Precipitation Climatology Centre (GPCC) data with the SSM weekly composites.

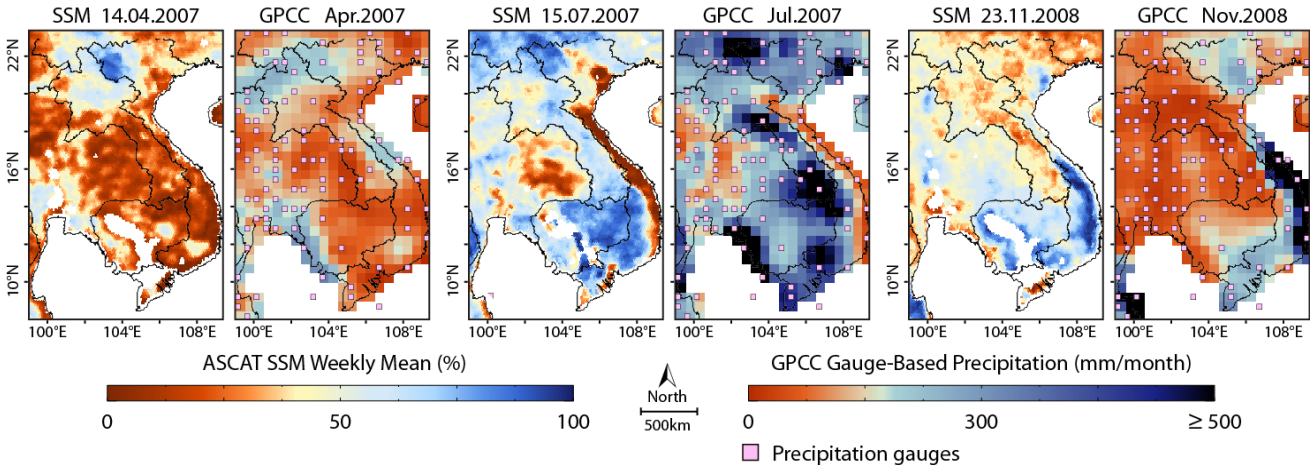

Figure 8. Comparison results of GPCC monthly anomalies and monthly soil moisture. r* shows critical correlation coefficient range considering significance level of $\alpha = 0.01$.

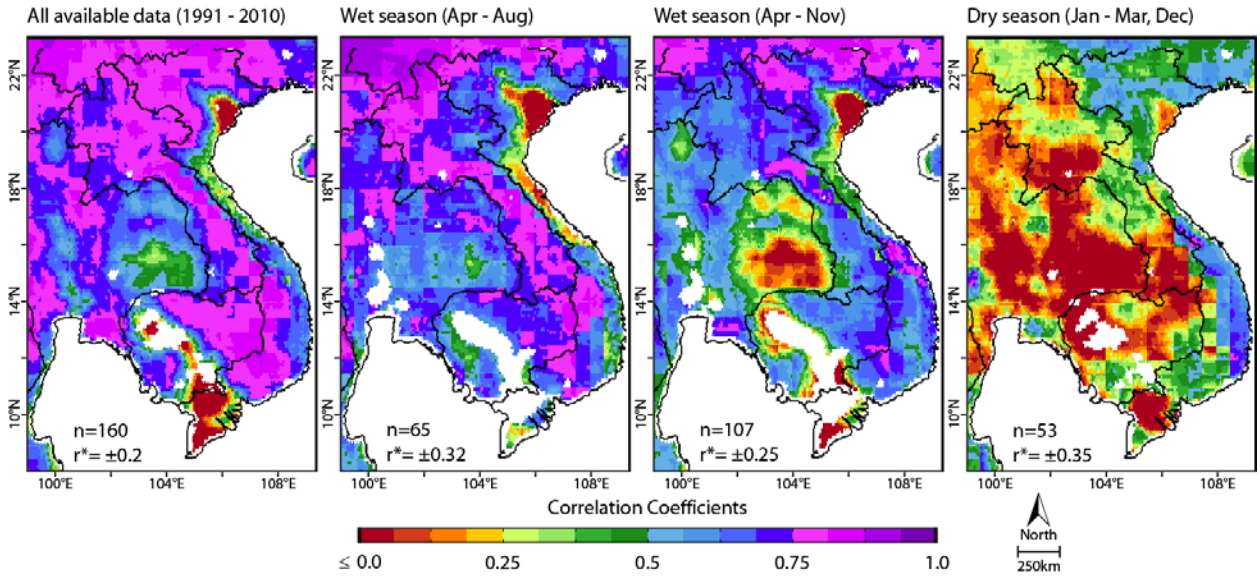

The correlation coefficients are significantly higher in wet season than in dry season. This is because of the specific regional climate of the LMB with distinctive dry season with no or very low precipitation. In agricultural areas especially in Delta region, Khorat plateau and northern Vietnam, correlation coefficients are clearly lower especially during dry season. In such regions the soil moisture regime does not always follow the meteorological conditions and other regional factors like irrigation activities have important influence on soil moisture conditions.

5.3. Spatiotemporal Variability of Soil Moisture in the LMB

5.3.1. Seasonal Variability of the BWI

Soil moisture conditions in the LMB are strongly influenced by the tropical monsoonal climate. The annual mean temperature in the LMB region varies just only few degrees between the hottest and coldest months of the year and the annual rainfall and evaporation are roughly equal over the major part of the basin. However, the variability of soil moisture is high throughout the LMB. Soil moisture patterns in the LMB are closely related to seasonal hydro-meteorological factors as well as the sub-catchments characteristics. The variability of soil moisture differs significantly, depending on region and month of the year, and changes year to year. Transition from dry to wet season in the LMB occurs in the period between March and May and transition from wet to dry season happens sometime between November and January [2]. The annual variability of normalized backscatter can be used for determination of the seasonal transition times. The transition times are calculated by using a least square fitting method of a step function applied on backscatter time series in the period of 2007–2010 [47]. According to this parameter, it can be seen in Figure 9 that the transition from dry to wet soil conditions in the LMB is observed foremost in the Delta region followed by in the agricultural regions in the northern Vietnam and southeastern Tonle Sap sub-catchments during the second half of March which is most likely related to irrigation activities. The onset of wet season begins in the Northern Highlands during April and in the rest of LMB sometime in May.

Figure 9. (**Left**) First and second transitions times determined based on the ASCAT annual backscatter variations. (**Right**) the annual backscatter at Ban Me Thout, Vietnam shown as an example.

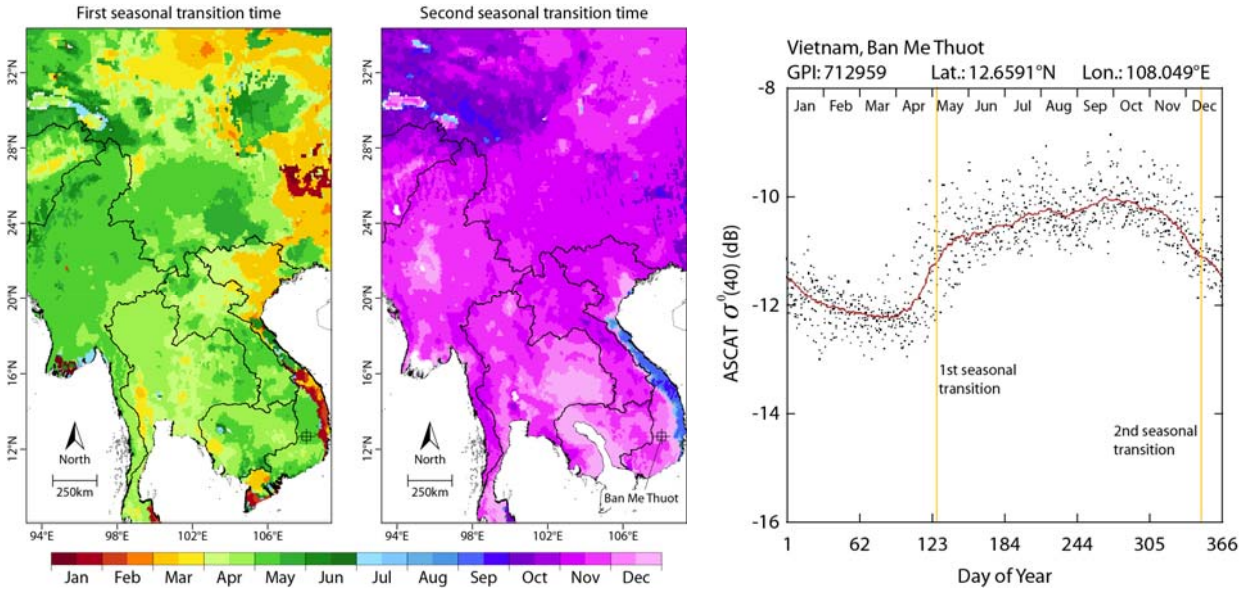

Monthly averages of the BWI for different sub-catchment areas calculated using the multi-year SSM time series indicate strong annual variability of soil moisture in the LMB. The wettest period across the LMB is from June to October and the driest months of the year are January to April (Figure 10). This corresponds to the fact that the total annual flow in the LMB occurs in an average year about 75% within just four months between July and October [48]. In December and January, the central and northern parts of the LMB are normally drier than the southern parts. March is the driest month across the LMB. During the wet season from May to September the BWI measurements show relatively drier conditions in Khorat plateau in Thailand compared to the other regions. In October the situation is reversed and the Nam Mun and Nam Chi sub-catchments in Thailand show wetter soil condition than the eastern and northeastern parts of the LMB in Laos. Decreasing of soil moisture in the LMB starts from the Northern Highlands in Laos during first weeks of November followed by other regions with delays of 1–2 weeks. The spatial distribution of the BWI reveals distinctive patterns throughout the LMB showing high variability of soil moisture between sub-catchments.

Figure 11(a,b) indicates total averages of BWI with and without considering flooding period and Figure 11(c) shows the standard deviation of the BWI calculated for each sub-catchment. Tropical monsoonal regions are generally associated with a water surplus and a highly reliable flow regime. Nevertheless, the BWI measurements indicated that the soil moisture condition still varies significantly in different parts of the LMB. The regions located in the north and the west of the LMB, show highest variability of soil moisture. The total mean of soil moisture is highest in the Northwestern mountainous regions of Laos, specifically in Nam Mae Kok, Nam Mae Kham, and Nam Mae Ing sub-catchments, as a result of higher rainfall and lower evaporation. The BWI values show a clear surplus of soil moisture in the south and the southeast regions of the LMB, Mekong Delta in Vietnam and the most parts of Cambodia, remarkably in Sre Pok, Se San, and the eastern Tonle Sap sub-catchments. There is also a decreasing gradient of soil moisture observable from east to west across the Mekong River within the

regions located in the central LMB. The highest evaporation occurs over the Khorat Plateau in northeast Thailand, one of the driest parts of Southeast Asia [2], which is also reflected in the soil moisture observations. In spite of significant soil moisture excess during the rainy season in summer, the total mean of soil moisture in this region is rather low compared to the other regions across the LMB. This implies that the area is particularly vulnerable to critically low levels of soil moisture during winter and has a high occurrence potential of agricultural drought conditions

Figure 10. Spatial maps of the monthly Basin Water Index (BWI) averaged over the periods between 1991–2000 and 2007–2011 illustrating the seasonal behavior of soil moisture in the Lower Mekong Basin (LMB).

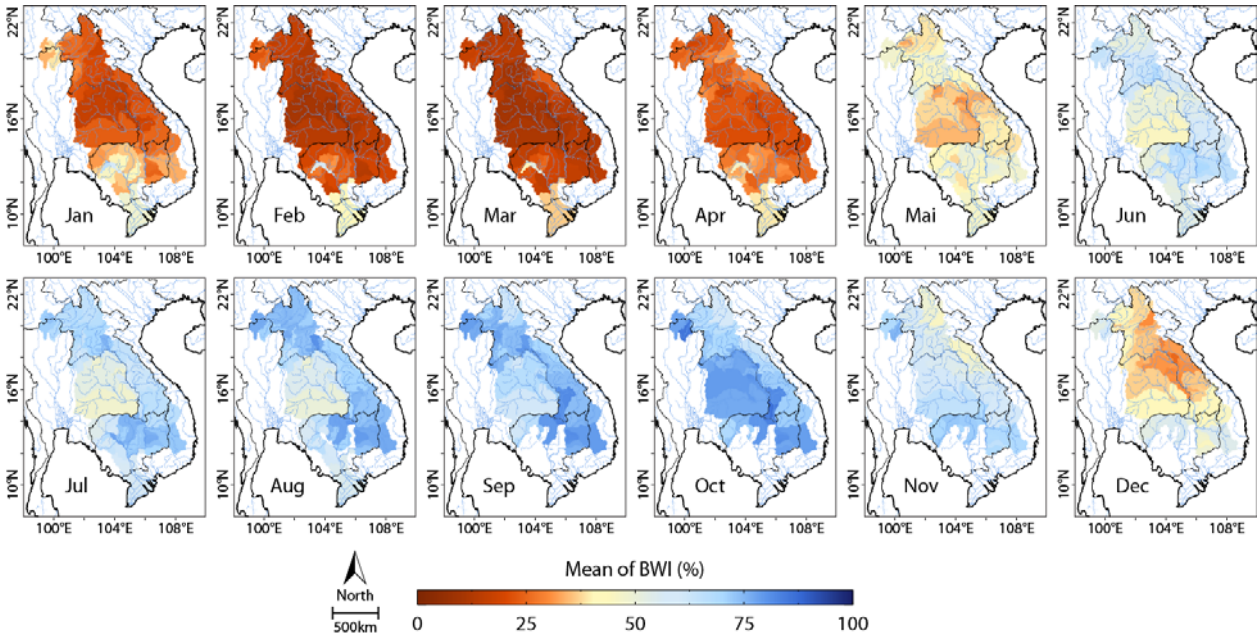

Figure 11. (**a**) Total mean of the calculated BWI; (**b**) Total Mean of the BWI after excluding flooding period; (**c**) Standard deviation of the BWI, during the periods of 1991–200 and 2007–2011.

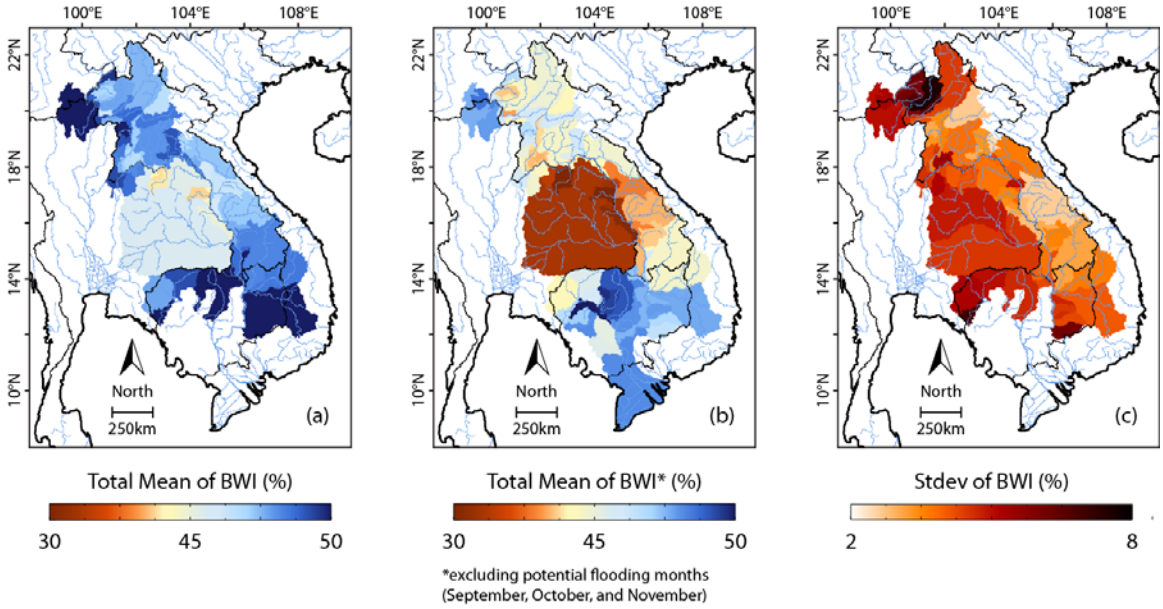

5.3.2. BWI Anomalies

The anomalies of BWI were calculated for all sub-catchments in the LMB using the total mean and standard deviation of soil moisture in catchment scale. Figure 12 illustrates the anomaly maps of BWI. Soil moisture retrieval is not possible during flooding period in Tonle Sap basin and Mekong Delta as the soil surface is usually covered largely with water. Therefore during the flooding period, the scatterometer measurements in these sub-catchments are excluded from the BWI anomaly calculation. Occurrence and location of the extreme events across the LMB differs each year depending on rainfall patterns and climate conditions. According to [2], there is no significant connection in the severity of the annual flood or drought between the northern and southern parts of the LMB, as the weather generating mechanisms which cause extreme conditions such as tropical storms and cyclones are usually not large enough to affect the region as a whole. The extreme wet conditions across the LMB between July and October are associated each year with a massive flood wave towards the LMB lowlands. During the flood season, water flows from the Mekong and Bassac rivers into the Tonle Sap Lake. From October onwards the flow direction is reversed and the water is drained back into the Mekong and Bassac rivers [49]. Each year, vast regions across the Cambodian lowlands and Vietnam delta are flooded for 2–4 months, affecting the life of several million people [50]. Analysis of the BWI time series in the periods of 1991–2000 and 2007–2011 showed that the years 1999 and 2000 were the wettest years. In 2000, severe flooding occurred with extended duration across the Cambodian lowlands and the Vietnam delta. The flooding event in 2000 led to over 800 fatalities, and economic damage exceeding 400 million USD [51]. Droughts in the LMB can occur at any time of the year. Extreme and prolonged dry conditions have considerable impacts on fisheries and agriculture. Unlike floods, droughts have no benefits and cause immense costs for the people living in the LMB. Droughts occur more often in Laos and Thailand (with the likelihood of two years in five) than in Cambodia and Vietnam (every three years) [2]. The BWI anomaly maps in 1992 show very dry conditions in the Thai sub-catchments (Nam Mun and Nam Chi) which are continued until 1993, predominantly in Nam Chi sub-catchment. The findings comply with hydro-meteorological observations at Vientiane and Kratie in Thailand. In the year 1992, the most severe drought since 1960 occurred when the peak and volume of the flood were 40 percent and more below the average figures [52]. The lowest BWI values in the Mekong Delta were observed in 1997–1998, 2007 and 2010. In 1998, the drought was equally profound in the LMB, especially in the Mekong Delta and the Tonle Sap basins. Tonle Sap lake did not expand as usual, with an estimated flooded area of 7,000 km² compared to a typical season maximum of 15,000 km² [2]. The BWI time series indicate that the year 2007 was a dry year in the whole LMB especially in Northern Highlands in Laos and northern Thailand. In 2010, extreme dry conditions were observable in the most parts of Laos, Cambodia, and the Mekong Delta. This is also confirmed with hydrological observations at Kratie. The total volume of flow at Kratie during the 2010 flood season was even less than that of 1992 which is generally regarded as the most severe drought on record [53]. The BWI anomalies show that the abnormal dry conditions in 2010 persisted until 2011 in the eastern Laos and the northern parts of the Tonle Sap basin.

Figure 12. Inter-annual anomalies of the BWI in the LMB.

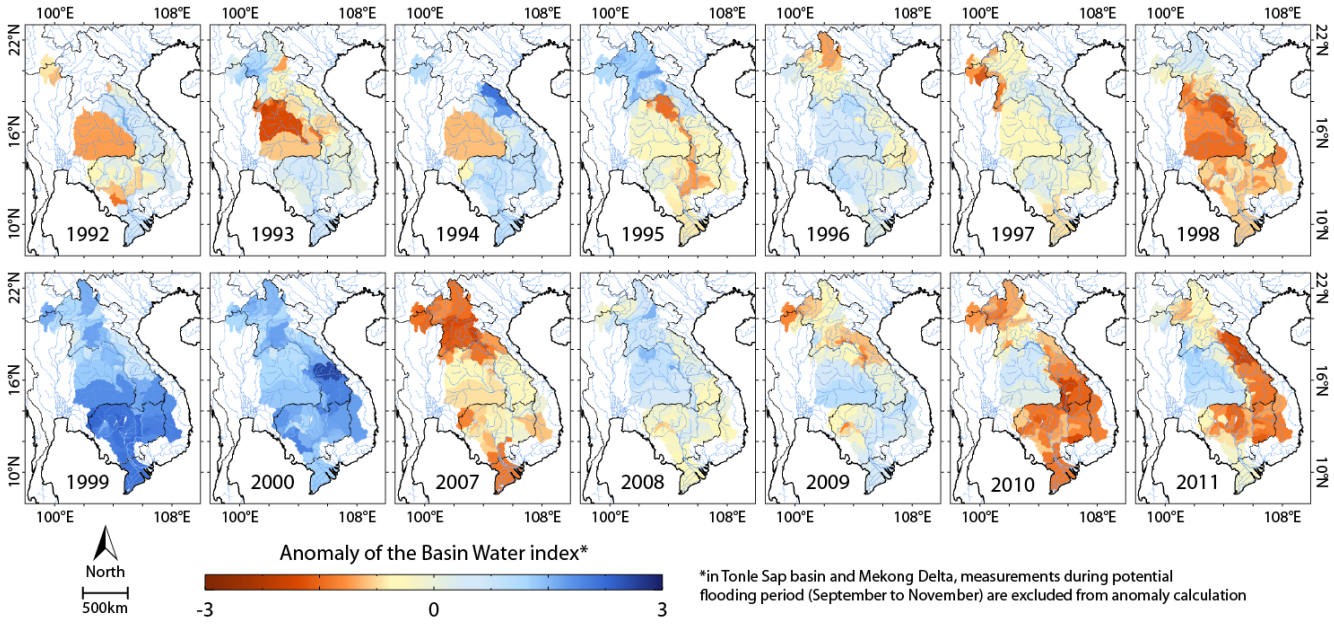

Figure 13. Comparison of the monthly BWI anomalies with Multivariate Enso Index (MEI): correlation coefficients are obtained by: (**a**) considering all measurements; and (**b**) considering only the measurements in May, during the periods of 1991–2000 and 2007–2011; (**c**) Comparison of the BWI and MEI measurements in May in Nam Chi sub-catchment, Thailand.

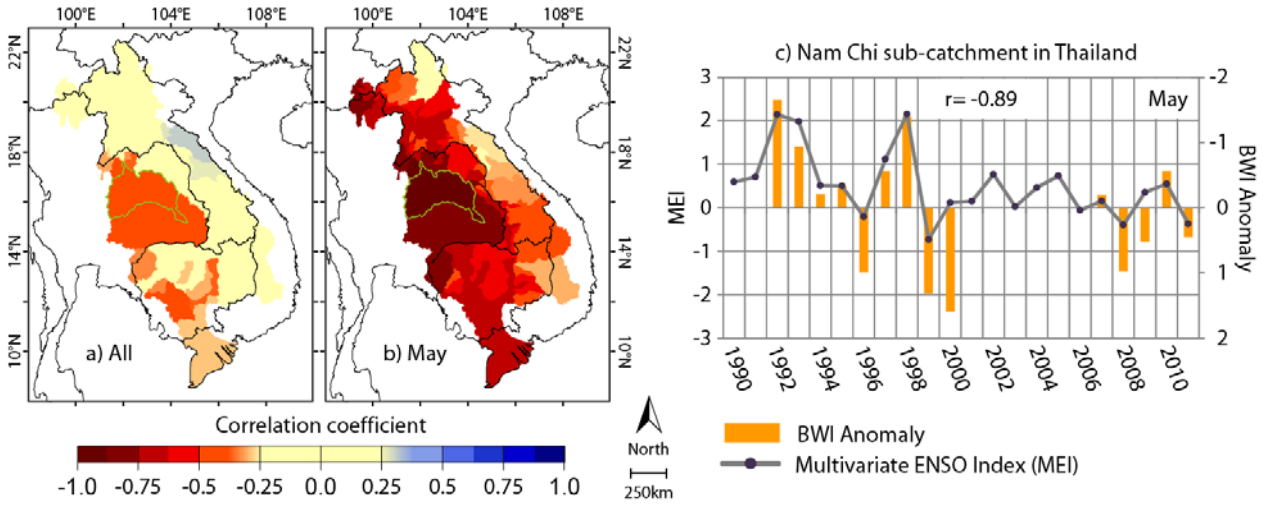

Many of the extreme droughts and floods in Southeast Asia are supposed to be associated with strong El Niño and La Niña events [53] as a result of the interaction between Asian Monsoon and El Niño Southern Oscillation (ENSO) [54–56]. Kuenzer *et al*. [57] demonstrated that the ENSO related climate variations in 1997/1998 are globally reflected in the scatterometer derived soil moisture data. To investigate the relation between the soil moisture extremes and ENSO events, the monthly BWI anomalies were compared with a Multivariate ENSO Index (MEI) dataset. The MEI used in this study is based on long-term marine measurements derived from tropical Pacific Comprehensive Ocean-Atmosphere Data Set (COADS) records and is a multivariate measure of the ENSO signal extracted from six observed variables over the tropical pacific: sea-level pressure, surface zonal and meridional

wind components, sea surface temperature, surface air temperature, and cloudiness [58,59]. Figure 13(a) illustrates the correlation coefficients calculated for each sub-catchment considering monthly BWI anomalies. There is a clear negative correlation between BWI anomalies and MEI in Khorat Plateau, Tonle Sap basin, and Mekong Delta. This finding corresponds to the observed link of the North-West Pacific monsoon, which in turn is influenced by ENSO, to the discharge in Kratie [60]. The correlation coefficients are markedly increased after performing the correlation analysis separately for each month of year, showing the strong seasonal relation of soil moisture and ENSO index. The most significant correlation was found in the period between April and June with the maximum in May (Figure 13(b)). Figure 13(c) shows time series of the BWI anomalies in May compared to MEI in Nam Chi sub-catchment in Thailand as example. In the catchments with low correlation coefficients, no conclusion could be made about the relation between BWI anomalies and MEI as the coefficients are statistically insignificant. However, in general, this might be due to low performance of the SSM retrieval in forest areas.

6. Summary and Conclusions

The scatterometer soil moisture retrieval showed satisfactory performance in most areas of the LMB with the exception of a few sub-catchments in the eastern parts of Laos, where the land cover is characterized by dense vegetation, and in areas with oversaturated soil situations induced by large flooding events in the Delta region and the Tonle Sap basin during the peak of wet season. The azimuthal noise, which causes uncertainties in the soil moisture retrieval, was generally low in most parts of the LMB with an average value of 0.18 dB (Figure 2(b)). The best performance of the retrieval algorithm was obtained in agricultural regions, shrubs, and grasslands with SSM noise less than five percent (Figure 2(c)), showing the high potential of the scatterometer derived soil moisture product for agricultural applications. Absolute validation of the SSM product was not possible as no long-term *in situ* soil moisture data are available in the LMB. However, despite the indirect relation of soil moisture and evaporation, comparison of the SSM time series with *in situ* evaporation data indicates significant inverse correlation up to $R = -0.85$ across the LMB, especially during the wet season. Comparison of the reanalysis precipitation anomalies with the SSM data showed also high correlation up to $R = 0.92$ especially in non-irrigated areas in the LMB.

In general, the spatiotemporal variability of soil moisture in the LMB was well captured by the SSM retrieval algorithm. The northern parts of the LMB in Laos and the west side of the Mekong River show the highest variations of soil moisture. The Mekong Delta, Tonle Sap basin and the northern parts of the LMB in Myanmar were identified as the wettest and the Thai sub-catchments in the LMB as the driest regions. The inter-annual variations of the BWI reveal distinct spatial patterns altering from year to year which are confirmed by the reported extreme hydro-meteorological events in the Mekong region. Furthermore, there was a clear indication that the ENSO related phenomena were contained in the BWI anomalies. The reasonable quality of the retrieved soil moisture in the LMB and the high-temporal acquisition capability of the European C-band scatterometers operating in all-weather conditions make the SSM product attractive for monitoring soil moisture dynamics in the LMB which is potentially valuable for numerous applications in hydrological and natural environmental processes such as climate studies, weather forecasting, runoff forecasting, soil erosion prediction, early flood warning, drought monitoring, irrigation planning, and yield monitoring.

Acknowledgments

This study was carried out in frame of WISDOM-II, Water related Information Management System for the Sustainable Development of the Mekong Delta, project funded by the German Ministry of Education and Research, BMBF.

References

1. Campbell, I. Introduction. In *The Mekong*; Ian, C.C., Ed.; Chapter 1; Academic Press: San Diego, CA, USA, 2009; pp. 1–11.
2. Mekong River Commission (MRC). *State of the Basin Report: 2010*; MRC: Vientiane, Lao PDR, 2010; p. 232.
3. Mekong River Commission (MRC). *State of the Basin Report: 2003*, *Executive Summary*; MRC: Phnom Penh, Cambodia, 2003; p. 50.
4. Mekong River Commission (MRC). *Annual Flood Report 2009*; MRC: Phnom Penh, Cambodia, 2009; p. 80.
5. Costa-Cabral, M.C.; Richey, J.E.; Goteti, G.; Lettenmaier, D.P.; Feldkotter, C.; Snidvongs, A. Landscape structure and use, climate, and water movement in the Mekong River basin. *Hydrol. Process.* **2008**, *22*, 1731–1746.
6. Kuenzer, C.; Campbell, I.; Roch, M.; Leinenkugel, P.; Tuan, V.Q.; Dech, S. Understanding the impact of hydropower developments in the context of upstream-downstream relations in the Mekong river basin. *Sustain. Sci.* **2012**, doi: 10.1007/s11625-012-0195-z.
7. Grayson, R.B.; Western, A.W.; Chiew, F.H.S.; Blöschl, G. Preferred states in spatial soil moisture patterns: Local and nonlocal controls. *Water Resour. Res.* **1997**, *33*, 2897–2908.
8. CEOS. *The Earth Observation Handbook*; Climate Change Special Edition: Noordwijk, The Netherlands, 2008.
9. Delworth, T.L.; Manabe, S. The influence of potential evaporation on the variabilities of simulated soil wetness and climate. *J. Clim.* **1988**, *1*, 523–547.
10. Reichle, R.H.; McLaughlin, D.B.; Entekhabi, D. Hydrologic data assimilation with the ensemble Kalman filter. *Mon. Wea. Rev.* **2002**, *130*, 103–114.
11. Robock, A.; Vinnikov, K.Y.; Srinivasan, G.; Entin, J.K.; Hollinger, S.E.; Speranskaya, N.A.; Liu, S.X.; Namkhai, A. The global soil moisture data bank. *Bull. Am. Meteorol. Soc.* **2000**, *81*, 1281–1299.
12. Famiglietti, J.S.; Devereaux, J.A.; Laymon, C.A.; Tsegaye, T.; Houser, P.R.; Jackson, T.J.; Graham, S.T.; Rodell, M.; van Oevelen, P.J. Ground-based investigation of soil moisture variability within remote sensing footprints during the Southern Great Plains 1997 (SGP97) hydrology experiment. *Water Resour. Res.* **1999**, *35*, 1839–1851.
13. Ulaby, F.T.; Fung, A.K.; Moore, R.K. *Microwave Remote Sensing: Active and Passive*; Addison-Wesley: Norwood, NJ, USA, 1982.
14. Leinenkugel, P.; Kuenzer, C.; Dech, S. Comparison and optimisation of MODIS cloud mask products for South East Asia. *Int. J. Remote Sens.* **2012**, in review.
15. Adamson, P.T.; Rutherfurd, I.D.; Peel, M.C.; Conlan, I.A. Chapter 4-The Hydrology of the Mekong River. In *The Mekong*; Ian, C.C., Ed.; Academic Press: San Diego, CA, USA, 2009; pp. 53–76.

16. Attema, E.P.W. The active microwave instrument on-board the ERS-1 satellite. *Proc. IEEE* **1991**, *79*, 791–799.
17. Figa-Saldana, J.; Wilson, J.J.W.; Attema, E.; Gelsthorpe, R.; Drinkwater, M.R.; Stoffelen, A. The Advanced Scatterometer (ASCAT) on the meteorological operational (MetOp) platform: A follow on for European wind scatterometers. *Can. J. Remote Sens.* **2002**, *28*, 404–412.
18. Wagner, W.; Lemoine, G.; Rott, H. A method for estimating soil moisture from ERS scatterometer and soil data. *Remote Sens. Environ.* **1999**, *70*, 191–207.
19. Naeimi, V.; Scipal, K.; Bartalis, Z.; Hasenauer, S.; Wagner, W. An Improved soil moisture retrieval algorithm for ERS and METOP scatterometer observations. *IEEE Trans. Geosci. Remote Sens.* **2009**, *47*, 1999–2013.
20. Wagner, W.; Bartalis, Z.; Naeimi, V.; Park, S.E.; Figa-Saldana, J.; Bonekamp, H. Status of the Metop ASCAT Soil Moisture Product. In Proceedings of the IEEE International Geosciences and Remote Sensing Symposium, Honolulu, HI, USA, 25–30 July 2010; pp. 276–279.
21. Naeimi, V.; Bartalis, Z.; Wagner, W. ASCAT soil moisture: An assessment of the data quality and consistency with the ERS scatterometer heritage. *J. Hydrometeorol.* **2009**, *10*, 555–563.
22. Mekong River commission (MRC). *Lower Mekong Basin Hydro Meteorology Database*; 2012. Available online: http://portal.mrcmekong.org/mastercatalogue/search?giai=9506000003818_E0200hvv (accessed on 1 February 2012).
23. Schneider, U.; Becker, A.; Finger, P.; Meyer-Christoffer, A.; Ziese, M.; Rudolf, B. GPCC's new land surface precipitation climatology based on quality-controlled in situ data and its role in quantifying the global water cycle. *Theor. Appl. Climatol.* **2013**, doi: 10.1007/s00704-013-0860-x.
24. Schneider, U.; Becker, A.; Finger, P.; Meyer-Christoffer, A.; Rudolf, B.; Ziese, M. *GPCC Full Data Reanalysis Version 6.0 at 0.5°: Monthly Land-Surface Precipitation from Rain-Gauges Built on GTS-Based and Historic Data*; GPCC: Main, Germany, 2011; doi: 10.5676/DWD_GPCC/FD_M_V6_050.
25. Ceballos, A.; Scipal, K.; Wagner, W.; Martinez-Fernandez, J. Validation of ERS scatterometer-derived soil moisture data in the central part of the Duero Basin, Spain. *Hydrol. Process.* **2005**, *19*, 1549–1566.
26. Parajka, J.; Naeimi, V.; Bloschl, G.; Wagner, W.; Merz, R.; Scipal, K. Assimilating scatterometer soil moisture data into conceptual hydrologic models at the regional scale. *Hydrol. Earth Syst. Sci.* **2006**, *10*, 353–368.
27. Scipal, K.; Drusch, M.; Wagner, W. Assimilation of a ERS scatterometer derived soil moisture index in the ECMWF numerical weal-her prediction system. *Adv. Water Resour.* **2008**, *31*, 1101–1112.
28. Zhao, D.; Kuenzer, C.; Fu, C.; Wagner, W. Evaluation of the ERS scatterometer-derived soil water index to monitor water availability and precipitation distribution at three different scales in China. *J. Hydrometeorol.* **2008**, *9*, 549–562
29. Liu, S.; Mo, X.; Zhao W.; Naeimi, V.; Dai, D.; Shu, C.; Mao, L. Temporal variation of soil moisture over the Wuding River basin assessed with an eco-hydrological model, *in situ* observations and remote sensing. *Hydrol. Earth Syst. Sci.* **2009**, *13*, 1375–1398.
30. Albergel, C.; Rüdiger, C.; Carrer, D.; Calvet, J.C.; Fritz, N.; Naeimi, V.; Bartalis, Z.; Hasenauer, S. An evaluation of ASCAT surface soil moisture products with *in situ* observations in Southwestern France. *Hydrol. Earth Syst. Sci.* **2009**, *13*, 115–124.

31. Brocca, L.; Melone, F.; Moramarco, T.; Wagner, W.; Naeimi, V.; Bartalis, Z.; Hasenauer, S. Improving runoff prediction through the assimilation of the ASCAT soil moisture product. *Hydrol. Earth Syst. Sci.* **2010**, *14*, 1881–1893.
32. Crow, W.T.; Wagner, W.; Naeimi, V. The impact of radar incidence angle on soil-moisture-retrieval skill. *IEEE Geosci. Remote Sens. Lett.* **2010**, *7*, 501–505.
33. Dorigo, W.A.; Scipal, K.; Parinussa, R.M.; Liu, Y.Y.; Wagner, W.; de Jeu, R.A.M.; Naeimi, V. Error characterisation of global active and passive microwave soil moisture datasets. *Hydrol. Earth Syst. Sci.* **2010**, *14*, 2605–2616.
34. Liu, Y.Y.; Parinussa, R.M.; Dorigo, W.A.; de Jeu, R.A.M.; Wagner, W.; van Dijk, A.I.J.M.; McCabe, M.F.; Evans, J.P. Developing an improved soil moisture dataset by blending passive and active microwave satellite-based retrievals. *Hydrol. Earth Syst. Sci.* **2011**, *15*, 425–436.
35. Naeimi, V.; Kuenzer, C.; Hasenauer, S.; Bartalis, Z.; Wagner, W. Evaluation of the Influence of Land Cover on the Noise Level of ERS-Scatterometer Backscatter. In Proceedings of the IEEE International Geosciences and Remote Sensing Symposium, Barcelona, Spain, 23–29 July 2007; pp. 3685–3688.
36. Wang, A.; Zeng, X.; Shen, S.S.P.; Zeng, Q.-C.; Dickinson, R.E. Time scales of land surface hydrology. *J. Hydrometeorol.* **2006**, *7*, 868–879.
37. Wagner, W.; Bloschl, G.; Pampaloni, P.; Calvet, J.C.; Bizzarri, B.; Wigneron, J.P.; Kerr, Y. Operational readiness of microwave remote sensing of soil moisture for hydrologic applications. *Nordic Hydrol.* **2007**, *38*, 1–20.
38. Bartholome, E.; Belward, A.S. GLC2000: A new approach to global land cover mapping from Earth observation data. *Int. J. Remote Sens.* **2005**, *26*, 1959–1977.
39. Kennett, R.G.; Li, F.K. Seasat over-land scatterometer data–II: Selection of extended area land-target sites for the calibration of spaceborne scatterometers. *IEEE Trans. Geosci. Remote Sens.* **1989**, *27*, 779–788.
40. Frison, P.-L.; Mougin, E. Use of ERS-1 wind scatterometer data over land surfaces. *IEEE Trans. Geosci. Remote Sens.* **1996**, *34*, 550–560.
41. Wagner, W.; Lemoine, G.; Borgeaud, M.; Rott, H. A study of vegetation cover effects on ers scatterometer data. *IEEE Trans. Geosci. Remote Sens.* **1999**, *37*, 938–948.
42. Macelloni, G.; Paloscia, S.; Pampaloni, P.; Santi, E. Global scale monitoring of soil and vegetation using SSM/I and ERS wind scatterometer. *Int. J. Remote Sens.* **2003**, *24*, 2409–2425.
43. US Geological Survey. *GTOPO30 Digital Elevation Model*; 1997. Available online: http://eros.usgs.gov/#/Find_Data/Products_and_Data_Available/gtopo30_info (accessed on 1 February 2007).
44. Delworth, T.L.; Manabe, S. The influence of potential evaporation on the variabilities of simulated soil wetness and climate. *J. Clim.* **1988**, *1*, 523–547.
45. Dirmeyer, P.A.; Schlosser, C.A.; Brubaker, K.L. Precipitation, recycling, and land memory: An integrated analysis. *J. Hydrometeorol.* **2009**, *10*, 278–288.
46. Hillel, D. *Introduction to Environmental Soil Physics*; Academic Press: Waltham, MA, USA, 2003.

47. Naeimi, V.; Paulik, C.; Bartsch, A.; Wagner, W.; Kidd, R.; Park, S.E.; Elger, K.; Boike, J. ASCAT Surface State Flag (SSF): Extracting information on surface freeze/thaw conditions from backscatter data using an empirical threshold-analysis algorithm. *IEEE Trans. Geosci. Remote Sens.* **2012**, *50*, 2566–2582.
48. Mekong River commission (MRC). *Overview of the Hydrology of the Mekong Basin*; MRC: Vientiane, Lao PDR, 2005; p. 73.
49. Lamberts, D. Little Impact, much Damage: The Consequences of Mekong River Flow Alterations for the Tonle Sap Ecosystem. In *Modern Myths of the Mekong: A Critical Review of Water and Development Concepts, Principles and Policies*; Kummu, M., Keskinen, M., Varis, O., Eds.; Helsinki University of Technology: Helsinki, Finland, 2008; pp. 3–18.
50. Mekong River commission (MRC). *Annual Flood Report 2009*; MRC: Phnom Penh, Cambodia, 2009; p. 80.
51. Nikula, J. Is Harm and Destructions all that Floods Bring? In *Modern Myths of the Mekong: A Critical Review of Water and Development Concepts, Principles and Policies*; Kummu, M., Keskinen, M., Varis, O., Eds.; Helsinki University of Technology: Helsinki, Finland, 2008; pp. 27–38.
52. Mekong River commission (MRC). *Annual Flood Report 2005*; MRC: Vientiane, Lao PDR, 2005; p. 82.
53. Mekong River commission (MRC). *Annual Flood Report 2010*; MRC: Phnom Penh, Cambodia, 2010; p. 76.
54. Ju, J.; Slingo, J. The Asian summer monsoon and ENSO. *Q. J. R. Meteorol. Soc.* **1995**, *121*, 1133–1168.
55. Wang, B.; Wu, R.; Fu, X. Pacific–East Asian teleconnection: How does ENSO affect East Asian climate? *J. Clim.* **2000**, *13*, 1517–1536.
56. Buckley, B.M.; Palakit, K.; Duangsathaporn, K.; Sanguantham, P.; Prasomsin, P. Decadal scale droughts over northwestern Thailand over the past 448 years: Links to the tropical Pacific and Indian Ocean sectors. *Clim. Dyn.* **2007**, *29*, 63–71
57. Kuenzer, C.; Zhao, D.; Scipal, K.; Sabel, D.; Naeimi, V.; Bartalis, Z.; Hasenauer, S.; Mehl, H.; Dech, S.; Wagner, W. El Niño southern oscillation influences represented in ERS scatterometer-derived soil moisture data. *Appl. Geogr.* **2009**, *29*, 463–477
58. Wolter, K.; Timlin, M.S. Monitoring ENSO in COADS with a Seasonally Adjusted Principal Component Index. In Proceedings of the 17th Climate Diagnostics Workshop, Norman, OK, USA, 1–5 November 1993; pp. 52–57.
59. Wolter, K.; Timlin, M.S. Measuring the strength of ENSO events: How does 1997/98 rank? *Weather* **1998**, *53*, 315–324.
60. Delgado, J.M.; Merz, B.; Apel, H. A climate-flood link for the lower Mekong River. *Hydrol. Earth Syst. Sci.* **2012**, *16*, 1533–1541.